



UNIVERSITÀ
DEGLI STUDI
DI PADOVA

Università degli Studi di Padova

Padua Research Archive - Institutional Repository

Au(III)-Proline derivatives exhibiting selective antiproliferative activity against HepG2/SB3 apoptosis-resistant cancer cells

Original Citation:

Availability:

This version is available at: 11577/3316323 since: 2019-11-29T09:15:09Z

Publisher:

Royal Society of Chemistry

Published version:

DOI: 10.1039/c9dt03036k

Terms of use:

Open Access

This article is made available under terms and conditions applicable to Open Access Guidelines, as described at <http://www.unipd.it/download/file/fid/55401> (Italian only)

(Article begins on next page)



Au(III)-proline derivatives exhibiting selective antiproliferative activity against HepG2/SB3 apoptosis-resistant cancer cells

L. Brustolin,^{a,b} N. Pettenuzzo,^{a,b} C. Nardon,^a S. Quarta,^c L. Marchiò,^d B. Biondi,^e P. Pontisso,^c D. Fregona^{*a}

Received 00th January 20xx,
Accepted 00th January 20xx

DOI: 10.1039/x0xx00000x

www.rsc.org/

This paper deals with the combination of a proline-based moiety with biologically active gold centers in the oxidation state +1 and +3. In particular, six Au(I)/(III)-proline dithiocarbamate (DTC) complexes, with general formulae $[\text{Au}^{\text{I}}_2(\text{DTC})_2]$ and $[\text{Au}^{\text{III}}\text{X}_2(\text{DTC})]$ (X=Cl, Br) are here reported. After the synthesis of the ligand and the complexes, all derivatives were characterized via several techniques, and tested for their stability in DMSO/water media. This study was focused on the demonstration of a peculiar behavior of Au(III)-DTC species in solution. Finally, the complexes were screened for their antiproliferative activity against 2 human cancer cell lines, namely HepG2 and HepG2/SB3, taken as a model of hepatocellular carcinoma. The latter, chosen for its aggressiveness due to the upregulation of the anti-apoptotic protein SerpinB3, was selectively inhibited in terms of growth by some Au(III)-DTC complexes.

Introduction

In recent years, gold-based coordination compounds, both in the oxidation states +1 and +3, have been extensively studied for their therapeutic applications as anticancer agents.^{1–5} Among them, in 2005 Fregona and coworkers discovered that gold-dithiocarbamate complexes are very promising in terms of *in vitro* and *in vivo* antiproliferative activity and toxicological profile.^{6,7} These compounds combine the anticancer properties of the gold center with the stabilizing properties of the chelating dithiocarbamate ligand (DTC).^{8,9} Consequently, the standard reduction potential of the couple Au(III)-Au(0) passes from +1.002 V for $[\text{AuCl}_4]^-$ to -0.22 V for $[\text{Au}(\text{DMDT})_2]^+$,^{6,10} consistent with a large stabilization of the +3 oxidation state upon coordination with DTC ligands. To date, a number of gold(I)/(III)-DTC derivatives have been synthesized and their biological profile revealed interesting perspectives in terms of activity also against cisplatin-resistant human cancer cell lines. For instance, gold(I)-DTC compounds of the type $[\text{Au}_2(\text{DTC})_2]$ ¹¹ and $[\text{Au}(\text{PR}_3)(\text{DTC})]$ ^{12–14} (PR_3 = phosphine) exhibited micromolar cytotoxicity IC_{50} values, with the latter involved in the DNA double helix distortion.¹⁴ On the other hand, gold(III)-DTC complexes showed outstanding preliminary results *in vivo*, both in terms of activity and toxicity. The sub-cutaneous injection of 1 mg kg^{-1} of

$[\text{AuBr}_2(\text{DMDT})]$ (DMDT= dimethyldithiocarbamate) every other day for 19 days to mice bearing androgen-resistant prostate cancer (PC3 cells) caused 85% tumor reduction.¹⁵ The studies on these complexes were followed by the synthesis of a “second generation” of Au(III)-DTC derivatives of the type $[\text{AuX}_2(\text{A}_1\text{A}_2\text{DTC})]$ (X=Cl, Br), where $\text{A}_1\text{A}_2\text{DTC}$ stands for an esterified peptide dithiocarbamate.¹⁶ These new derivatives were designed to achieve a cancer-selective drug delivery and an improved intracellular uptake, by exploiting the transporters PEPT1 and PEPT2, mammalian membrane proteins, overexpressed in certain types of tumors.¹⁷ The *in vivo* experiments in nude mice bearing the triple negative MDA-MB-231 breast tumor, with $[\text{Au}^{\text{III}}\text{Br}_2(\text{dte-A}_1\text{-A}_2\text{-O}(\text{t-Bu}))]$ (A_1 = sarcosine; A_2 = Aib (aminoisobutyric acid)), showed a 53% of tumor growth inhibition compared to control (1 mg kg^{-1} day⁻¹ after a 27-day treatment). Interestingly, for both the first and second generation complexes, the evaluation of the acute toxicity, followed by histological analysis of the major organs, were very hopeful.^{16,18–20} In a more recent work we substituted sarcosine by L-proline as A_1 unit in the dipeptide chain, to give rigidity to the dithiocarbamic moiety chelating the Au(III) center. The screenings on some cancerous cell lines demonstrated that the resulting complexes exhibit antiproliferative activities similar to – or, in some cases, higher than – cisplatin.²¹ To better investigate the effect mediated by the L-proline moiety on the cytotoxic properties of the gold-DTC compounds, in this work we synthesized and tested both Au(I) and Au(III) derivatives of the L-proline ester dithiocarbamate. We screened our novel compounds for their antiproliferative activity against the HepG2 cell line (human hepatocellular carcinoma), and the apoptosis-resistant HepG2/SB3 counterpart (human hepatocellular carcinoma overexpressing the anti-apoptotic protein SerpinB3).²² This amino acid is particularly interesting because a L-proline-based ligand has been already explored to achieve a selective delivery of the cytotoxic unit to aggressive tumors²³, and 3D-growing cancer cells have been demonstrated to be associated with a large consume of proline from the culture medium.²⁴ Finally,

^a Department of Chemical Sciences, University of Padova, Via F. Marzolo 1, 35131 Padova (Italy)

^b Department of Surgical, Oncologic and Gastroenterological Sciences, University of Padova, Via Giustiniani 2, 35128, Padova (Italy)

^c Department of Medicine, University of Padova, Via Giustiniani 2, 35128, Padova (Italy)

^d Department of Chemical Sciences, Life Sciences and Environmental Sustainability, Parco Area delle Scienze 11/a, 43124, Parma (Italy)

^e CNR, Padova Unit, Inst Biomol Chem, Via Marzolo 1, I-35131 Padua, Italy

*Corresponding author's e-mail: dolores.fregona@unipd.it

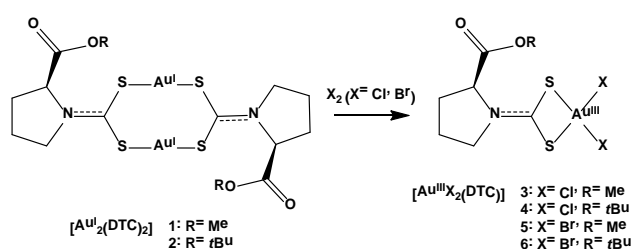
Electronic Supplementary Information (ESI) available: this file contains contains the experimental spectra (FT-IR, ¹H-NMR and UV-Vis) of the synthesized compounds. See DOI: 10.1039/x0xx00000x

L-proline has been used *in vivo* as targeting agent in ^{99m}Tc -based tumor imaging.²⁵

Results and discussion

Synthetic routes

In this work we focused on the oxidative addition of halides (Br_2 and Cl_2) to dinuclear Au(I) precursors with stoichiometry $[\text{Au}_2(\text{DTC})_2]$ in halogenated solvent for obtaining complexes of the type $[\text{AuX}_2(\text{DTC})]$, according to Blaauw and coworkers (Scheme 1).²⁶ The Au(I)-DTC derivatives were obtained by fast *in situ* NaAuCl_4 reduction with Na_2SO_3 of, followed by the addition of DTC ligand.²⁷ The syntheses of the L-proline DTCs were performed according to a literature procedure, under anhydrous conditions (N_2 atmosphere, dry methanol) and using a sterically-hindered base (NaOtBu) to avoid the hydrolysis of the $-\text{OR}$ group ($\text{R} = \text{Me}$, $t\text{Bu}$) of the L-proline esters.²⁸



Scheme 1 The oxidative addition of halogen (Cl_2 or Br_2) to the dinuclear gold(I) precursors $[\text{Au}^{\text{I}}_2(\text{DTC})_2]$ (left) led to the neutral gold(III) complexes of the type $[\text{Au}^{\text{III}}\text{X}_2(\text{DTC})]$ (right).

X-ray structural analysis

The compounds **4** (CCDC 1845775) and **6** (CCDC 1845777), presented in Fig. 1 and 3, respectively, are isostructural and they exhibit very similar structural features to those of **5** (CCDC 1845776), shown in Fig. 2. In particular, the asymmetric unit comprises two independent molecules, which differ in the orientation of the ester group with respect to the plane of the dithiocarbamate ligand. In these three structures, the metal is in a square planar geometry bound by the bidentate dithiocarbamate and by two halide anions.

Focusing on the bond lengths (see Table SI 2 in the ESI file), the Au-S distances are shorter in the case of dichloro-derivative (ca. 2.30 Å) with respect to the dibromo counterparts (ca. 2.32 Å). This is owed to the slightly greater trans-influence exerted by the bromide ion with respect to the chloride one.²⁹ Moreover, the length of the C-N bond in all complexes (ca. 1.30 Å) results closer to values known for the C=N bond (1.32 Å) than the C-N bond (1.47 Å),³⁰ thus highlighting the prevalence of the thioureidic form for the proline dithiocarbamates.²⁸ Finally, the two independent molecules of the asymmetric unit are stacked one over the other, establishing two distinct Au...S contacts between the two molecules (3.53-3.68 Å range). The molecular structure of the complexes 4-6 with thermal ellipsoids drawn at the 50% probability level are reported in Fig. SI 1, Fig. SI 2, Fig. SI 3.

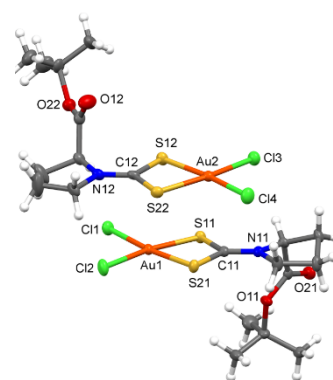


Fig. 1 Molecular structure of the complex **4** with thermal ellipsoids drawn at the 30% probability level. Both molecular entities within the asymmetric unit are shown. CCDC 1845775.

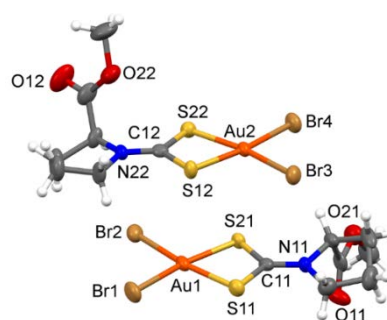


Fig. 2 Molecular structure of the complex **5** with thermal ellipsoids drawn at the 30% probability level. Both molecular entities within the asymmetric unit are shown. CCDC 1845776.

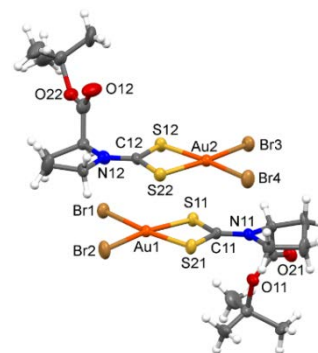


Fig. 3 Molecular structure of the complex **6** with thermal ellipsoids drawn at the 30% probability level. Both molecular entities within the asymmetric unit are shown. CCDC 1845777.

FT-IR characterization

The IR spectra of the ligands and compounds **1-6** are reported in Fig. SI 4-17 in the ESI file. Three fundamental IR-regions must be taken into account when studying transition metal-dithiocarbamate complexes, whose bands corresponding to stretching vibration modes (ν):^{31,32}

- between 1200 and 1550 cm^{-1} , backbone $\nu_{\text{SSC-N}}$ vibration;
- between 950-1050 cm^{-1} and 550-650 cm^{-1} , $\nu_{\text{a}}(\text{C-S})$ and $\nu_{\text{s}}(\text{C-S})$ respectively;

- between 300 and 470 cm^{-1} , $\nu(\text{Au-S})$ vibration.

The **Table 1** summarizes the diagnostic bands of the synthesized compounds. For the $\nu(\text{SSC-N})$ vibration, the following trend is found: $[\text{Au}^{\text{III}}\text{X}_2(\text{DTC})] > [\text{Au}^{\text{I}}_2(\text{PipeDTC})_2] > \text{DTC salt}$. In agreement with what observed by Calbro and co-workers on Au(II)-DTC derivatives, the $\nu(\text{SSC-N})$ frequency of the DTC ligand increases as the oxidation state of gold rises.³³ In particular, the obtained values reflect a thioureidic form of the ligand, with a partial double character of the C-N bond, as suggested by the crystallographic studies. Moreover, the presence of a single band associated with this vibration mode clearly indicates that the dithiocarbamate groups coordinate the metal ion in a single way. Concerning the second diagnostic region ascribed to the C-S stretching mode, the presence of only a band in the region 950 and 1050 cm^{-1} (corresponding to the asymmetric C-S stretching) points out a symmetric bidentate coordination of the ligand.³⁴ Finally, the **Table 1** highlights the Au-S bond is stronger in gold(I) derivatives. Indeed, the Au-S frequency increases as the oxidation number of the metal center decreases, owed to a reduced possibility of the gold(III) ion to back-donate π electron density to the DTC ligand.³⁵

Compound	$\nu(\text{N-C})$	$\nu_a(\text{CSS})$	$\nu_s(\text{CSS})$	$\nu_a(\text{Au-S})$	$\nu_s(\text{Au-S})$
NaProOMeDTC	1392 cm^{-1}	945 cm^{-1}	-	-	-
NaProOtBuDTC	1388 cm^{-1}	933 cm^{-1}	-	-	-
1	1418 cm^{-1}	950 cm^{-1}	553 cm^{-1}	452 cm^{-1}	-
2	1412 cm^{-1}	965 cm^{-1}	536 cm^{-1}	444 cm^{-1}	-
3	1560 cm^{-1}	979 cm^{-1}	547 cm^{-1}	382 cm^{-1}	339 cm^{-1}
4	1558 cm^{-1}	950 cm^{-1}	545 cm^{-1}	381 cm^{-1}	341 cm^{-1}
5	1550 cm^{-1}	985 cm^{-1}	546 cm^{-1}	378 cm^{-1}	349 cm^{-1}
6	1560 cm^{-1}	953 cm^{-1}	541 cm^{-1}	379 cm^{-1}	345 cm^{-1}

Table 1 Collection of diagnostic IR-vibrations (4000-100 cm^{-1}) of the synthesized proline DTC salts and the corresponding Au(I)/Au(III) complexes.

¹H-NMR characterization

The ¹H-NMR spectra of the ligands recorded in MeOD and compounds **1-6**, recorded DMSO-*d*₆, are reported in the **Fig. SI 18-25**. The spectra of the gold(I) precursors **1** and **2** have a low signal-to-noise ratio due to the poor solubility of these complexes in all deuterated solvents. However, the ¹H-NMR spectroscopy allowed us to check the progression of the oxidation reaction by comparison with the spectra of the Au(I)/Au(III) derivatives.

Comparing the chemical shifts of all complexes with those of the free dithiocarbamate ligands, a lower-field shift of the signals related to the α -protons to the dithiocarbamic nitrogen atom, is detected after coordination. Concerning the neutral Au(III)-DTC coordination compounds the *H*(α)-signals of the chloro-derivatives are found at slightly lower fields with respect to the bromo-counterparts, due to the higher electronegativity of the former. On the contrary, the presence of the halogen as well as the +3 oxidation state of the metal center does not affect, or affects to a small extent, the resonance of the other protons of the ligand, if compared to those of Au(I) derivatives. Finally, the -OR group (R= methyl, *tert*-butyl) signal confirms the absence of hydrolysis side-reactions during the oxidative addition reaction.

UV-Vis studies

These studies were carried out in DMSO for the poorly soluble Au(I) compounds, and in CH_2Cl_2 for the Au(III)-DTC counterparts (the spectra are reported in the **Fig. SI 26-31**). The summary of the bands is highlighted in **Table SI 3** and the related discussion is in the supporting information³⁶⁻⁴³.

The complexes **1-6** were also studied for their stability in DMSO/H₂O mixture in 1:9 ratio. Indeed, due to their poor water solubility, to carry out *in vitro* antiproliferative studies the complexes were pre-dissolved in sterile-filtered DMSO just before the experiments. According to the **Fig. SI 32-33** (800-200 nm), the Au(I)-DTC compounds resulted stable over 72, with no spectral change during this period. Concerning the Au(III) complexes, the **Fig. 4** shows the UV-Vis stability study of the compound **5** in DMSO/H₂O 1:9, over 72 h as an example (for the others see the **Fig. SI 34-36**). The initial neutral compound is completely converted to a new one in 4 hours, and the corresponding electronic spectrum possesses the characteristic camel-hump shape of $[\text{Au}(\text{DTC})_2]^+$ complexes,⁴⁴ as reported by Isab and coworkers in a recent work.⁴⁵

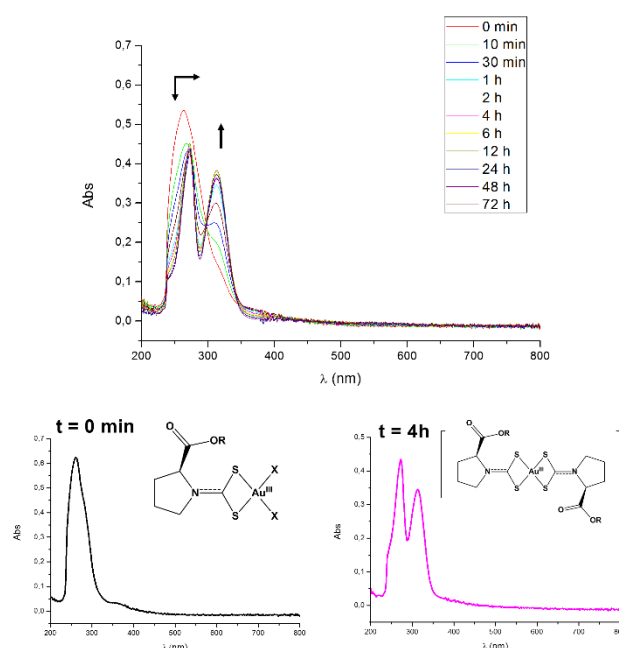


Fig. 4 The UV-Vis analysis over 72 hours of the compound **5** dissolved in DMSO/H₂O 1:9 at 37 °C (top). The observed behavior is clearer if comparing the spectrum at *t* = 0 (pure $[\text{AuBr}_2(\text{ProOMeDTC})]$), with the one at *t* = 4 h, which shows the classic spectral shape of $[\text{Au}(\text{DTC})_2]^+$ derivatives.⁴⁵ (bottom)

The presence of this equilibrium implies that the ionic 1:2 species formed in cell medium, when the cells are treated with the neutral 1:1 complexes. Intriguingly, this behavior was not observed during the ¹H-NMR characterization in DMSO-*d*₆, and the samples were stable for many days in presence of light. This contradictory phenomenon is currently under investigation, but it is probably related to an isotopic effect mediated by deuterium. Indeed, during the substitution reaction of square planar complexes, the solvent plays a crucial role in the stabilization of the intermediates, acting as a ligand.⁴⁶ Thus, the presence of deuterium instead of hydrogen can interfere with the coordination capability of DMSO, thus hampering the conversion from the neutral 1:1 to ionic 1:2 Au(III) complex.

Anticancer activity

For testing the antiproliferative activity of the investigated compounds, human tumor cell lines HepG2 and HepG2/SB3 cells were exposed to different concentrations of all the metal-DTC complexes (*i.e.*, 10 μM , 5 μM , 2 μM , 1 μM , 0.5 μM and in some cases lower) for 72 hours. To avoid the possibility that the effect of the compounds on cell viability would be affected by the presence of proline, the cytotoxicity tests were also carried out in presence of complete medium containing proline at 1, 10, and 100 $\mu\text{g/ml}$ concentration. As reported in **Fig. SI 39**, the presence of proline does not influence the cytotoxicity of the compounds. Quadruplicate conditions were established for each treatment and at least three independent experiments were carried out for each compound. We set 10 μM as experimental IC_{50} cut-off, given that we consider higher values not useful for a future pharmaceutical development.

Concerning the hepatocellular carcinoma, one of the most spread malignances worldwide, the studies were focused on the HepG2 cell line and its more aggressive HepG2/SB3 counterpart. The latter is associated with resistance to oncological treatments due to the overexpression of the anti-apoptotic protein SerpinB3.⁴⁷ Indeed, this serine-protease inhibitor is typically found in cancer cells of epithelial origin, and significantly attenuates apoptosis triggered by anti-cancer drugs or TNF- α , thus allowing tumor growth.⁴⁸ Moreover, this protein locates in the inner mitochondrial compartments, where it binds to the respiratory *Complex I*, protects cells from the pro-oxidant action of some chemotherapeutic agents, such as doxorubicin and cisplatin.⁴⁹

The **Table 2** summarizes the IC_{50} values collected for the compounds 1-6, the proline-based DTC and the metal precursor $\text{NaAuCl}_4 \cdot 2\text{H}_2\text{O}$. For comparison purposes, the cytotoxicity of cisplatin (dissolved in saline solution) was evaluated under the same experimental conditions.

Compound	IC_{50} (μM)	
	HepG2	HepG2/SB3
$\text{NaAuCl}_4 \cdot 2\text{H}_2\text{O}$	> 10	> 10
NaProOMeDTC	> 10	> 10
NaProOtBuDTC	> 10	> 10
1	> 10	> 10
2	> 10	> 10
3	> 10	3.52 \pm 0.04
4	> 10	5.6 \pm 0.2
5	> 10	7.14 \pm 0.06
6	> 10	5.5 \pm 0.2
Cisplatin	> 10	> 10

Table 2 IC_{50} values (μM) calculated after a 72-h treatment (concentration of the test agent inducing 50% reduction in cell number compared with control cell cultures). Data represent the mean \pm SD of at least three independent experiments (Vehicle: DMSO for compounds 1-6; saline solution for DTC ligands, cisplatin and the Au(III) precursor).

Neither the ligand salts, nor the Au(III) commercially available precursor resulted cytotoxic towards the tested cell cultures. Similarly, Au(I)-DTC derivatives resulted inactive, thus confirming previous anticancer studies on $[\text{Au}'_2(\text{DTC})_2]$ complexes, which were associated with a low cytotoxic activity *in vitro*.¹¹ As designed, the antiproliferative activity springs from the combination of the DTC ligand with a gold center in oxidation state +3. In particular, although complexes 3-6 lack of activity toward HepG2 line, they show a good degree of selectivity, being able to overcome the resistance to apoptosis induced by SerpinB3.

CD preliminary studies

The function of a protein or peptide is closely related to its structure. Since circular dichroism measurements probe protein structure changes, CD is widely used for the structural analysis of protein formulated for pharmaceutical use. CD spectral shapes reflect the abundance ratio of secondary structure motifs in proteins and secondary structure analysis of CD data provides a fast and thorough indication of changes in these structures.⁵⁶

Considering that the complexes 3-6 showed an evident selectivity for the HepG2/SB3 cells overexpressing Serpin, we investigated if the compounds were able to interact with the SB3 native protein carrying out some preliminary CD experiments over time at 37°C. The most active complex 3 was solubilized in CDCl_3 and added to a buffered solution of serpin protein in 1:1 and 1:100 (SB3: complex 3) molar ratios. The results reported in **Fig. SI 37** and in **Table SI 4** showed that the addition of complex 3 is accompanied by some evident changes in the protein structure which tend to be minimized over time. In 24 h the structure of the protein seems to restore. This behaviour could be ascribable to a direct non-denaturing and reversible interaction of the complex with the protein, but other experiments must be carried out to assess the real significance of that interaction. For comparison purposes the same experiments were performed with the non-active compounds 1 and 2 showing non interaction with SB3 native protein allowing to assess that the non-covalent interaction with the protein could be significant in the selectivity of the active complexes. For clarity reasons, only the curves after 2 and 4 hours related to the experiment at 1:100 molar ratio are reported in figure SI 34.

Experimental

General Experimental Details

All reagents and solvents for chemical syntheses were purchased from Merck and Alfa Aesar. Elemental analyses were carried out at the Microanalysis Laboratory of the Department of Chemical Sciences, University of Padova by a microanalyzer Fisons EA-1108 CHNS-O and a microanalyzer Carlo Erba 1108 CHNS-O. ESI-MS spectra were recorded by a Mariner Perspective Biosystem instrument, in the positive mode setting a 5-kV ionization potential and a 20 $\mu\text{L/min}$ flow rate. A mixture of coumarin and 6-methyltryptophan was used as a standard. Samples were dissolved in methanol (used also as eluent). ESI-MS spectra have been processed by the software Data Explorer. Near FT-IR spectra (4000-400 cm^{-1}) were recorded at room temperature (32 scans, resolution 2 cm^{-1}) by Nicolet Nexus 55XC spectrophotometer. KBr pellets of samples were prepared according to standard procedures. Far FT-IR spectra (600-50 cm^{-1}) were acquired at room temperature with a

Nicolet Nexus 870 spectrophotometer. For the analysis, films of the sample dispersed in nujol were loaded into polyethylene discs (250 scans, resolution 4 cm⁻¹). Spectra were processed with OMNIC 5.2 (Nicolet Instrument Corporation). ¹H-NMR spectra of metal-DTC complexes were recorded at 298 K with a Bruker Avance DRX300 spectrometer equipped with a BBI [1H, X] probe-head, Bruker. Typical acquisition parameters for 1D ¹H-NMR spectra (1H: 300.13 MHz): normal pulse sequence, 64 transients, spectral width 15 ppm using a delay time of 1.0 sec. The data sets were processed with the standard Bruker processing software package Topspin 1.3. Chemical shifts were referenced to solvent signal. Peak assignment and integral calculations were carried out by means of MestReNova (version 6.2.0, Mestrelab Research S.L.). Absorption spectra of freshly-prepared solutions of the samples were acquired at 25 and 37 °C in the range 200-800 nm with an Agilent Cary 100 UV-Vis double beam spectrophotometer, taking into account the solvent cut-off. Samples were dissolved in the proper solvents and the resulting solutions were placed in QS quartz cuvettes (path length 1 cm).

Syntheses and Characterizations

Synthesis of the L-proline ester dithiocarbamate sodium salts (Na DTC)

The proline-based DTC ligands were synthesized according to literature procedures.²⁸

L-proline methyl ester dithiocarbamate sodium salt, Na ProOMeDTC
Aspect: white hygroscopic solid. Yield: 80%. Mp.: n.d. ¹H-NMR (CD₃OD, 300.13 MHz): δ (ppm) = 2.03-2.33 (m, 4H, H₍₃₎ + H₍₄₎), 3.69 (s, 3H, O-CH₃), 3.95 (m, 2H, H₍₅₎), 5.07-5.11 (dd, 1H, H₍₂₎). Medium FT-IR (KBr): $\tilde{\nu}$ (cm⁻¹) = 2953.03 (ν_a, C-H); 1733.20 (ν, C=O); 1392.38 (ν_a, N-CSS); 1177.76 (ν_a, C-OMe); 944.78 (ν_a, CSS); 504.45 (ν_s, CSS). ESI-MS *m/z*, [DTC] found (calc.): 204.03 (204.02). Anal. Calc. for C₇H₁₀NNaO₂S₂ (MW = 227.28 g·mol⁻¹): C 36.99; H 4.43; N 6.16; S 28.22. Found: C 36.93; H 4.32; N 6.11; S 28.30.

L-proline tert-butyl ester dithiocarbamate sodium salt, Na ProOtBuDTC

Aspect: beige hygroscopic solid. Yield: 71%. Mp.: n.d. ¹H-NMR (CD₃OD, 300.13 MHz): δ (ppm) = 1.47 (s, 9H, O-C(CH₃)₃), 2.01-2.30 (m, 4H, H₍₃₎ + H₍₄₎), 3.94 (m, 2H, H₍₅₎), 4.97-4.99 (dd, 1H, H₍₂₎). Medium FT-IR (KBr): $\tilde{\nu}$ (cm⁻¹) = 2974.63 (ν_a, C-H); 1722.65 (ν, C=O); 1388.27 (ν_a, N-CSS); 1151.18 (ν_a, C-OtBu); 932.89 (ν_a, CSS); 502.02 (ν_s, CSS). ESI-MS *m/z*, [DTC] found (calc.): 246.07 (246.06). Anal. Calc. for C₁₀H₁₆NNaO₂S₂ (MW = 269.36 g·mol⁻¹): C 44.59; H 5.99; N 5.20; S 23.81. Found: C 44.50; H 5.91; N 5.25; S 23.90.

Synthesis of the gold(I)-DTC complexes of the type [Au^I₂(DTC)₂] 1-2

The gold(I) complexes of the proline ester dithiocarbamate ligands were obtained starting from a gold(I) solution, freshly prepared by dissolving 1 mmol of NaAuCl₄·2H₂O in NaCl saturated water (10 mL) followed by the reduction Au(III)→Au(I) with 1 mmol of Na₂SO₃ at 0 °C under stirring. When the solution turned from orange (Au^{III}) into colorless (Au^I), immediately 1 mmol (1 eq) of the dithiocarbamate salt, dissolved in water (5 mL), was added, leading to the instantaneous formation of a solid product. The mixture was left under vigorous stirring for 5 minutes, and then the precipitate was centrifuged, washed three times with 5 mL of water and dried in vacuum in the presence of P₂O₅.

Bis(L-proline methyl ester dithiocarbamate)digold(I), [Au₂(ProOMeDTC)₂], 1

Aspect: beige solid. Yield: 83%. Mp.: 220 °C (dec.). ¹H-NMR (DMSO-d₆, 300.13 MHz): δ (ppm) = 2.06 (m, 8H, H₍₃₎ + H₍₄₎), 3.69 (s, 6H, O-CH₃), 3.82-3.89 (m, 4H, H₍₅₎), 4.94 (s, 2H, H₍₂₎). Medium FT-IR (KBr): $\tilde{\nu}$ (cm⁻¹) = 2952.82 (ν_a, C-H); 1738.78 (ν, C=O); 1418.46 (ν_a, N-CSS); 1158.52 (ν_a, C-OMe); 950.14 (ν_a, CSS). Far FT-IR (nujol): $\tilde{\nu}$ (cm⁻¹) = 552.59 (ν_s, CSS); 452.10 (ν_a, Au-S). Anal. Calc. for C₁₄H₂₀Au₂N₂O₄S₄ (MW = 802.51 g·mol⁻¹): C 20.95; H 2.51; N 3.49; S 15.98. Found: C 21.12; H 2.64; N 3.38; S 15.92.

Bis(L-proline tert-butyl ester dithiocarbamate)digold(I), [Au₂(ProOtBuDTC)₂], 2

Aspect: beige solid. Yield: 81%. Mp.: 208 °C (dec.). ¹H-NMR (DMSO-d₆, 300.13 MHz): δ (ppm) = 1.45 (s, 18H, O-C(CH₃)₃), 2.10 (m, 8H, H₍₃₎ + H₍₄₎), 3.84-3.91 (m, 4H, H₍₅₎), 4.98 (s, 2H, H₍₂₎). Medium FT-IR (KBr): $\tilde{\nu}$ (cm⁻¹) = 2973.43 (ν_a, C-H); 1733.78 (ν, C=O); 1412.10 (ν_a, N-CSS); 1156.90 (ν_a, C-OtBu); 964.82 (ν_a, CSS). Far FT-IR (nujol): $\tilde{\nu}$ (cm⁻¹) = 535.91 (ν_s, CSS); 444.31 (ν_a, Au-S). Anal. Calc. for C₂₀H₃₂Au₂N₂O₄S₄ (MW = 886.67 g·mol⁻¹): C 27.09; H 3.64; N 3.16; S 14.17. Found: C 27.28; H 3.72; N 3.11; S 14.32.

Synthesis of the gold(III)-DTC complexes of the type [Au^{III}X₂(DTC)] (X=Cl, Br) 3-6

0.5 mmol of gold(I)-DTC complex were suspended in 20 mL of halogenated solvent (chloroform or dichloromethane) and the mixture was refluxed under stirring. For the chloro-derivatives, after 10 minutes an excess of Cl₂ (generated in a separate flask by mixing 300 mg of MnO₂ with 3 mL of concentrated HCl) was gurgled for 20 minutes, observing that the solution turned brown with the dissolution of the Au(I) precursor, and then became yellow. The bromo-complexes were obtained with an excess of bromine, directly added to the Au(I)-DTC suspension (100 equivalents of liquid Br₂ previously dissolved in dichloromethane), and the solution turned immediately intense red, and then orange. Both reactions were refluxed in presence of the halogen (Cl₂ or Br₂) for 1 h, then the flask was cooled, the mixture filtered and the volume of the solvent half-reduced. Afterwards, 40 mL of diethyl ether were added, leading to the precipitation of a solid that was filtered, washed with 2x 4 mL of diethyl ether and 2x 5 mL of distilled water, and dried in pump in the presence of P₂O₅.

Dichloro(L-proline methyl ester dithiocarbamate)gold(III), [AuCl₂(ProOMeDTC)], 3

Aspect: orange solid. Yield: 89%. Mp.: 175 °C. ¹H-NMR (DMSO-d₆, 300.13 MHz): δ (ppm) = 2.01-2.40 (4m, 4H, H₍₃₎ + H₍₄₎), 3.76 (s, 3H, O-CH₃), 3.92-4.01 (2m, 2H, H₍₅₎), 5.16-5.17 (dd, 1H, H₍₂₎). Medium FT-IR (KBr): $\tilde{\nu}$ (cm⁻¹) = 2951.38 (ν_a, C-H); 1746.56 (ν, C=O); 1559.95 (ν_a, N-CSS); 1173.93 (ν_a, C-OMe); 979.24 (ν_a, CSS). Far FT-IR (nujol): $\tilde{\nu}$ (cm⁻¹) = 546.77 (ν_s, CSS); 381.91 (ν_a, Au-S); 359.01 (ν_a, Au-Cl); 339.07 (ν_s, Au-S); 318.79 (ν_s, Au-Cl). Anal. Calc. for C₇H₁₀AuCl₂NO₂S₂ (MW = 472.16 g·mol⁻¹): C 17.81; H 2.13; N 2.97; S 13.58. Found: C 17.86; H 2.22; N 2.90; S 13.65.

Dichloro(L-proline tert-butyl ester dithiocarbamate)gold(III), [AuCl₂(ProOtBuDTC)], 4

Aspect: yellow-orange needles. Yield: 86%. Mp.: 160 °C (dec.). ¹H-NMR (DMSO-d₆, 300.13 MHz): δ (ppm) = 1.45 (s, 9H, O-C(CH₃)₃), 1.97-2.40 (4m, 4H, H₍₃₎ + H₍₄₎), 3.92-3.99 (2m, 2H, H₍₅₎), 5.01-5.02 (dd, 1H, H₍₂₎). Medium FT-IR (KBr): $\tilde{\nu}$ (cm⁻¹) = 2975.38 (ν_a, C-H); 1737.74 (ν, C=O); 1558.38 (ν_a, N-CSS); 1146.04 (ν_a, C-OtBu); 950.15

(ν_a , CSS). Far FT-IR (nujol): $\tilde{\nu}$ (cm^{-1}) = 545.20 (ν_s , CSS); 380.68 (ν_a , Au-S); 358.23 (ν_a , Au-Cl); 341.14 (ν_s , Au-S); 319.14 (ν_s , Au-Cl). Anal. Calc. for $\text{C}_{10}\text{H}_{16}\text{AuCl}_2\text{NO}_2\text{S}_2$ (MW = 514.24 $\text{g}\cdot\text{mol}^{-1}$): C 23.36; H 3.14; N 2.72; S 12.47. Found: C 23.50; H 3.05; N 2.60; S 12.65.

Dibromo(L-proline methyl ester dithiocarbamate)gold(III), [AuBr₂(ProOMeDTC)], 5

Aspect: orange needles. Yield: 91%. Mp.: 157 °C. ¹H-NMR (DMSO-*d*₆, 300.13 MHz): δ (ppm) = 2.00-2.41 (4m, 4H, H₍₃₎ + H₍₄₎), 3.76 (s, 3H, O-CH₃), 3.91-3.99 (2m, 2H, H₍₅₎), 5.13-5.15 (dd, 1H, H₍₂₎). Medium FT-IR (KBr): $\tilde{\nu}$ (cm^{-1}) = 2949.35 (ν_a , C-H); 1746.46 (ν , C=O); 1550.36 (ν_a , N-CSS); 1173.25 (ν_a , C-OMe); 985.14 (ν_a , CSS). Far FT-IR (nujol): $\tilde{\nu}$ (cm^{-1}) = 544.59 (ν_s , CSS); 378.26 (ν_a , Au-S); 349.40 (ν_s , Au-S); 237.49 (ν_a , Au-Br); 219.92 (ν_s , Au-Br). Anal. Calc. for $\text{C}_7\text{H}_{10}\text{AuCl}_2\text{NO}_2\text{S}_2$ (MW = 561.06 $\text{g}\cdot\text{mol}^{-1}$): C 14.98; H 1.80; N 2.50; S 11.43. Found: C 15.12; H 1.79; N 2.36; S 11.56.

Dibromo(L-proline tert-butyl ester dithiocarbamate)gold(III), [AuBr₂(ProOtBuDTC)], 6

Aspect: orange needles. Yield: 90%. Mp.: 216 °C (dec.). ¹H-NMR (DMSO-*d*₆, 300.13 MHz): δ (ppm) = 1.45 (s, 9H, O-C(CH₃)₃), 1.98-2.38 (m, 4H, H₍₃₎ + H₍₄₎), 3.89-3.97 (m, 2H, H₍₅₎), 4.98-5.00 (dd, 1H, H₍₂₎). Medium FT-IR (KBr): $\tilde{\nu}$ (cm^{-1}) = 2977.36 (ν_a , C-H); 1736.46 (ν , C=O); 1559.96 (ν_a , N-CSS); 1146.69 (ν_a , C-OtBu); 952.67 (ν_a , CSS). Far FT-IR (nujol): $\tilde{\nu}$ (cm^{-1}) = 540.70 (ν_s , CSS); 379.35 (ν_a , Au-S); 344.53 (ν_s , Au-S); 238.34 (ν_a , Au-Br); 219.02 (ν_s , Au-Br). Anal. Calc. for $\text{C}_{10}\text{H}_{16}\text{AuCl}_2\text{NO}_2\text{S}_2$ (MW = 603.14 $\text{g}\cdot\text{mol}^{-1}$): C 19.91; H 2.67; N 2.32; S 10.63. Found: C 20.02; H 2.70; N 2.29; S 10.71.

Crystallographic studies

The slow precipitation of compounds **4**, **5**, and **6** in dichloromethane/diethyl ether yielded yellow-orange needles suitable for crystallographic studies. A summary of data collection and structure refinement is reported in Table SI 1. Single crystal data were collected with a Bruker Smart Breeze, a Bruker Smart APEXII and a Bruker D8 venture PhotonII, Mo K α : λ = 0.71073 Å. The intensity data were integrated from several series of exposures frames (0.3° width) covering the sphere of reciprocal space (SMART (control) and SAINT (integration) software for CCD systems; Bruker (2012) - Bruker AXS Inc., Madison, Wisconsin, USA). Absorption correction was applied using the program SADABS.⁵⁰ The structures were solved by the dual space algorithm implemented in the SHELXT code⁵¹ or by direct methods using SIR2004.⁵² Fourier analysis and refinement were performed by the full-matrix least-squares methods based on F² implemented in SHELXL-2014.⁵³ Graphical material was prepared with the Mercury 3.9 program.⁵⁴

Biological studies

In vitro model

In vitro tests were conducted using the HepG2 cell line (LGC Standards), stably transfected with the plasmid vector pCDNA3.1 carrying the SerpinB3 human gene (these cells hereinafter identified as HepG2/SB3 cells), and, in parallel, the HepG2 cell line transfected with the empty vector (hereinafter identified as HepG2/CTR cells, where CTR stands for "control"), using Lipofectamin (Invitrogen). Cells were cloned by serial dilution and expanded using G418 selective medium. Transfection was performed according to the manufacturer's instructions.⁵⁵ HepG2/CTR and HepG2/SB3 cells were separately cultured in Minimum Essential Medium (MEM), with addition of FBS (10%), L-

glutamine (2 mM), MEM non-essential amino acid (1%), streptomycin (100 $\mu\text{g}/\text{mL}$), and penicillin (100 units/mL), 0.3mg/ml of G418 as selective agent and incubated at 37 °C in a 5% carbon dioxide controlled atmosphere.

The cellular model was characterized for SERPINB3 expression by analyzing the expression of SERPINB3 in transfected clones by immunofluorescence and real-time PCR. (Fig. SI 38)

Immunofluorescence

The expression of SERPINB3 in transfected cells was assessed by immunofluorescence. Cells were seeded on slides (2×10^5 HepG2 cells/slide) and cultured for 48 h. After fixation with 4% paraformaldehyde, permeabilized with 0.2% Tryton X100, the cells were blocked with 5% BSA in PBS. The slides were incubated with 8 $\mu\text{g}/\text{ml}$ rabbit polyclonal antibody (Hepa-Ab, Xeptagen), washed with 0.1% Tween 20 in phosphate-buffered saline (PBS) and incubated with anti-rabbit Alexa Fluor 546 secondary antibody (1 : 500 dilution, Invitrogen). Cellular nuclei were counter-stained with DAPI (Sigma-Aldrich). The slides were mounted with ELVANOL (Sigma-Aldrich) and observed under a fluorescence microscope (Axiovert 200M, Carl Zeiss MicroImaging GmbH) using Apotome.2 optical sectioning system.

Real-Time PCR

Total RNA was isolated from transfected HepG2 cells using RNeasy Mini Kit (Qiagen), according to the manufacturer's instructions. SerpinB3 mRNAs levels were measured by quantitative Real-Time PCR (DNA Engine Opticon2, MJ Research) using SYBR Green PCR Master Mix (Applied Biosystems) and specific sets of primers (SerpinB3-F: 5'-aactcctgggtggaagtgaa-3'; SerpinB3-R: 5'-accaatgtgtattctgctgcaa-3'). Relative gene expression was normalized to the housekeeping gene glyceraldehyde-3-phosphate dehydrogenase (GAPDH, F: 5'-TGGTATCGTGGAAGGACTCATGAC-3'; R: 5'-ATGCCAGTGAGCTTCCCGTTCAGC-3') and was calculated using the 2^{- $\Delta\Delta\text{CT}$} method.

Cytotoxicity studies

For the cytotoxicity assay, the transfected cells were trypsinized and seeded in 96-well microplates ($4 \cdot 10^4$ cells/well) in the complete growth medium (200 μL), and incubated at 37 °C in a 5% CO₂ atmosphere for 24 h to allow cell adhesion. Then were treated for 72 hours with vehicle (control; namely DMSO) or each compound (pre-dissolved in the vehicle) in fresh medium at the defined concentrations (i.e., 10 μM , 5 μM , 2 μM , 1 μM , 0.5 μM). The cytotoxicity tests were also carried out at the same concentration of the compounds in complete medium containing 1, 10, and 100 $\mu\text{g}/\text{ml}$ of proline. Cell viability was evaluated via MTT assay, according the standard procedures.

Circular Dichroism (CD)

The CD curves were recorded on a Jasco (Tokyo, Japan) model J-1500 spectropolarimeter equipped with a Haake thermostat (Thermo Fisher Scientific, Waltham, MA). Baselines were corrected by subtracting the solvent contribution. A fused quartz cell of 0.2 mm pathlength (Hellma, Germany) was employed. The values are expressed in terms of $[\theta]_T$, the total molar ellipticity ($\text{deg} \times \text{cm}^2 \times \text{dmol}^{-1}$). The protein was diluted with a HEPES (4-(2-hydroxyethyl)-1-piperazineethanesulfonic acid) 5 mM, pH 7.4 buffer solution. The

complex 3 was solubilized in CDCl₃ before adding it to the buffered solution of the SB3 protein in 1:1 and 1:100 molar ratios (SB3: Complex 3). Even if the DMSO was used to solubilize the complex before treating the cells, it was not possible to use it for this experiment because of its range of absorption which blinds the instrument below 200 nm. The final amount of CDCl₃ in solution was kept within 1% to avoid damaging the protein structure.

Conclusions

The first goal of this work was the synthesis of novel Au(I)/Au(III) compounds stabilized by proline-based DTC ligands. The choice of this amino acid lies on its generally recognized ability to selectively deliver the cytotoxic unit into aggressive cancer cells. In particular, we focused our attention on the methyl- and *tert*-butyl esters of L-proline to avoid off-target coordination of the metal center to the carboxylic function, act as a driver of the cytotoxic unit towards aggressive cancer cells.

The dithiocarbamate ligands and their complexes of the type [Au^I₂(DTC)₂] and [Au^{III}X₂(DTC)] (X= Cl, Br) were characterized by means of elemental analysis, X-ray crystallography (complexes 4-6), ESI-MS, ¹H-NMR spectroscopy, FT-IR and UV-Vis spectrophotometry.

The UV-Vis stability studies of compounds 3-6 in DMSO-H₂O highlighted a particular solution behavior since neutral Au(III)-DTC complexes undergoes a process of conversion to the ionic form [Au(DTC)₂]⁺, when dissolved in polar media such as DMSO and water.

The synthesized complexes have been screened for their biological activity towards human hepatocellular carcinoma cells. The results have pointed out that only the Au(III) derivatives possess IC₅₀ values lower than our selected cut-off of 10 μM. In particular, they are endowed with a selectivity of action against HepG2/SB3, very aggressive cells over-expressing the anti-apoptotic protein SerpinB3. For the complex 3 this phenomenon is more evident, and future studies will elucidate its mechanism of action and the role of the proline moiety in terms of cell uptake.

Conflicts of interest

There are no conflicts to declare.

Notes and references

- J.-J. Zheng, W. Lu, R. W.-Y. Sun, C.-M. Che, *Angew. Chem. Int. Ed.*, 2012, **51**, 4882.
- C. Nardon, G. Boscutti, L. Dalla Via, P. Ringhieri, V. Di Noto, G. Morelli, A. Accardo, D. Fregona, *Med. Chem. Comm*, 2015, **6**, 155.
- T. Zou, C. T. Lum, C.-N. Lok, J.-J. Zhang, C.-M. Che, *Chem. Soc. Rev.*, 2015, **44**, 8786.
- C. Nardon, N. Pettenuzzo, D. Fregona, *Curr. Med. Chem.*, 2016, **23**, 3374.
- A. Casini, R. W.-Y. Sun, I. Ott, *Met. Ions Life Sci.* 2018, **18**, doi: 10.1515/9783110470734-013.
- L. Ronconi, L. Giovagnini, C. Marzano, F. Bettio, R. Graziani, G. Pilloni, D. Fregona, *Inorg. Chem.*, 2005, **44**, 1867.
- C. Nardon, G. Boscutti, D. Fregona, *Anticancer Res.*, 2014, **34**, 487.
- V. Milacic, D. Fregona, Q. P. Dou, *Histol. Histopathol.*, 2008, **23**, 101.
- D. Fregona, L. Ronconi, *Dalton Trans.*, 2009, **48**, 10670.
- A. A. Mohamed, A. E. Bruce, M. R. M. Bruce in *The electrochemistry of gold and silver complexes* (Patai's chemistry of functional groups), John Wiley & Sons, 2009.
- A. A. Sulaiman, M. Altaf, A. A. Isab, A. Alawad, S. Altuwajiri, S. Ahmad, Z. Anorg. *Allg. Chem.*, 2016, **642**, 1454.
- F. K. Keter, I. A. Guzei, M. Nell, W. E. van Zyl, J. Darkwa, *Inorg. Chem.*, 2014, **53**, 2058.
- M. Altaf, M. Monim-ul-Mehboob, A. A. A. Seliman a, M. Sohail, M. I. M. Wazeer, A. A. Isab, L. Li, V. Dhuna, G. Bhatia, K. Dhuna, *Eur. J. Med. Chem.*, 2015, **95**, 464.
- S. S. Al-Jaroudi, M. Altaf, A. A. Seliman, S. Yadav, F. Arjmand, A. Alhoshani, H. M. Korashy, S. Ahmad, A. A. Isab, *Inorg. Chim. Acta*, 2017, **464**, 37.
- L. Cattaruzza, D. Fregona, M. Mongiat, L. Ronconi, A. Fassina, A. Colombatti, D. Aldinucci, *Int. J. Cancer*, 2011, **128**, 206.
- C. Nardon, D. Fregona, *Curr. Top. Med. Chem.*, 2016, **16**, 360.
- C. U. Nielsen, B. Brodin, F. S. Jorgensen, S. Frokjaer, B. Steffansen, *Expert Opin. Ther. Patents*, 2002, **12**, 1329.
- C. Marzano, L. Ronconi, F. Chiara, M. C. Giron, I. Faustinelli, P. Cristofori, A. Trevisan, D. Fregona, *Int. J. Cancer*, 2011, **129**, 487.
- M. Celegato, D. Fregona, M. Mongiat, L. Ronconi, C. Borgese, V. Canzonieri, N. Casagrande, C. Nardon, A. Colombatti, D. Aldinucci, *Fut. Med. Chem.*, 2014, **6**, 1249.
- C. Nardon, S. M. Schmitt, H. Yang, J. Zuo, D. Fregona, Q. P. Dou, *Plos ONE*, 2014, **9**, e84248.
- G. Boscutti, C. Nardon, L. Marchiò, M. Crisma, B. Biondi, D. Dalzoppo, L. Dalla Via, F. Formaggio, A. Casini, D. Fregona, *ChemMedChem*, 2018, **13**, 1131.
- P. Pontisso, *Ann. Hepatol.*, 2014, **13**, 722.
- J. M. Phang, W. Liu, C. N. Hancock, J. W. Fischer, *Curr. Opin. Clin. Nutr. Metab. Care*, 2015, **18**, 71.
- I. Elia, D. Broekaert, S. Christen, R. Boon, E. Radaelli, M. F. Orth, C. Verfaillie, T. G. P. Grünwald, S.-M. Fendt, *Nat. Commun.*, 2017, **8**, 15267.
- M. Liu, X. Lin, X. Song, Y. Cui, P. Li, X. Wang, J. Zhang, *J. Radioanal. Nucl. Chem.*, 2013, **298**, 1659.
- H. J. A. Blaauw, R. J. F. Nivard, G. J. M. Van Der Kerk, *J. Organomet. Chem.*, 1964, **2**, 236.
- R. Hesse, P. Jennische, *Acta Chem. Scand.*, 1972, **26**, 3855.
- L. Brustolin, C. Nardon, N. Pettenuzzo, N. Zuin Fantoni, . Quarta, F. Chiara, A. Gambalunga, A. Trevisan, L. Marchiò, P. Pontisso, D. Fregona, *Dalton Trans.*, 2018, **47**, 15477.
- F. A. Cotton, G. Wilkinson in *Advanced Inorganic Chemistry*, Wiley, 1988.
- Handbook of Chemistry and Physics (85th ed.), D. R. Lide ed., CRC Press, London (UK), 2004.
- D. A. Brown, W. K. Glass, M. A. Burke, *Spectrochim. Acta Mol. Biomol. Spectrosc.*, 1976, **32**, 137.
- F. Forghieri, G. Graziosi, C. Preti, G. Tosi, *Transit. Met. Chem.*, 1983, **8**, 372.
- D. C. Calabro, B. A. Harrison, G. Todd Palmer, M. K. Moguel, R. L. Rebbert, J. L. Burmeister, *Inorg. Chem.*, 1981, **20**, 4311.
- F. Bonati, R. Ugo, Organotin(IV) N, N-disubstituted dithiocarbamates, *J. Organomet. Chem.*, 1967, **10**, 257.
- H. O. Desseyn, A. C. Fabretti, F. Forghieri, C. Preti, *Spectrochim. Acta A*, 1985, **41**, 1105.
- C. C. Hadjikostas, G. A. Katsoulos, S. K. Shakatreh, *Inorg. Chim. Acta*, 1987, **133**, 129.
- R. Narayanaswamy, M. A. Young, E. Parkhurst, M. Ouellette, M. E. Kerr, M. H. Douglas, R. C. Elder, A. E. Bruce, M. R. M. Bruce, *Inorg. Chem.*, 1993, **32**, 2506.
- H.-R. Jaw, M. M. Savas, W. R. Mason, *Inorg. Chem.*, 1989, **28**, 4366.
- H. B. Gray, C. J. Ballhausen, *Inorg. Chem.*, 1963, **85**, 260.

- 40 W. R. Mason III, H. B. Gray, *Inorg. Chem.*, 1968, **7**, 55.
- 41 D.H. Brown, G. C. McKinlay, W.E. Smith, *Inorg. Chim. Acta*, 1979, **32**, 117.
- 42 A. K. Gangopadhyay, A. Chakravorty, *J. Chem. Phys.*, 1961, **35**, 2206.
- 43 F. Forghieri, C. Preti, L. Tassi, G. Tosi, *Polyhedron*, 1988, **7**, 1231.
- 44 P. T. Beurskens, H. J. A. Blaauw, J. A. Cras, J. J. Steggerda, *Inorg. Chem.*, 1968, **7**, 805.
- 45 M. Altaf, A. A. Isab, J. Vanco, Z. Dvorak, Z. Travnicek, H. Stoeckli-Evans, *RCS Adv.*, 2015, **5**, 81599.
- 46 E. J. Billo, *Inorg. Chem.*, 1973, **12**, 2783.
- 47 L. Vidalino, A. Doria, S. Quarta, M. Zen, A. Gatta, P. Pontisso, *Autoimmun. Rev.*, 2009, **9**, 108.
- 48 C. Turato, A. Vitale, S. Fasolato, M. Ruvoletto, L. Terrin, S. Quarta, R. Ramirez-Morales, A. Biasiolo, G. Zanus, N. Zali, P. S. Tan, Y. Hoshida, A. Gatta, U. Cillo, P. Pontisso, *Br. J. Cancer*, 2014, **110**, 2708.
- 49 F. Ciscato, M. Sciacovelli, G. Villano, C. Turato, P. Bernardi, A. Rasola, P. Pontisso, *Oncotarget*, 2014, **5**, 2418.
- 50 L. Krause, R. Herbst-Irmer, G. M. Sheldrick and D. Stalke, *J. Appl. Crystallog.*, 2015, **48**, 3.
- 51 G. M. Sheldrick, *Sect. A Found. Crystallogr.*, 2015, **71**, 3.
- 52 M. C. Burla, R. Caliendo, M. Camalli, B. Carrozzini, G. L. Cascarano, C. Giacovazzo, M. Mallamo, A. Mazzone, G. Polidori, R. Spagna, *J. Appl. Crystallog.*, 2012, **45**, 357.
- 53 G. M. Sheldrick, *Acta crystallogr., C Struct. Chem.*, 2015, **71**, 3.
- 54 C. F. Macrae, P. R. Edgington, P. McCabe, E. Pidcock, G. P. Shields, R. Taylor, M. Towler and J. Van De Streek, *J. Appl. Crystallog.*, 2006, **39**, 453.
- 55 S. Quarta, L. Vidalino, C. Turato, M. Ruvoletto, F. Calabrese, M. Valente, S. Cannito, G. Fassina, M. Parola, M. Gatta and P. Pontisso, *J. Pathol.*, 2010, **221**, 343.
- 56 J. Reed and T. A. Reed, *Anal. Biochem.*, 1997, **254**, 36.